AD-A281 573

||||||||||||||||||||||||||||||||

RL-TR-94-68
Final Technical Report
April 1994

HIGH-EFFICIENCY ELECTRO-OPTIC GRATING ON PLZT CERAMIC WAFER FOR OPTICAL SWITCHING

Syracuse University

Q. Wang Song

DTIC
ELECTE
JUL 1 4 1994
S   D

DTIC QUALITY INSPECTED 5

94-21574

||||||||||||||||||||||||||||||||

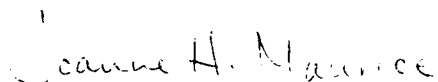**Rome Laboratory**
Air Force Materiel Command
Griffiss Air Force Base, New York

94 7 12 2 57

This report has been reviewed by the Rome Laboratory Public Affairs Office (PA) and is releasable to the National Technical Information Service (NTIS). At NTIS it will be releasable to the general public, including foreign nations.
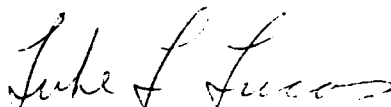
RL-TR-94-68 has been reviewed and is approved for publication.

APPROVED: _Joanne H. Maurice_

JOANNE H. MAURICE
Project Engineer

FOR THE COMMANDER _Luke L. Lucas_

LUKE L. LUCAS, Colonel, USAF
Deputy Director
Surveillance & Photonics

REPORT DOCUMENTATION PAGE

Form Approved
OMB No. 0704-0188

1. AGENCY USE ONLY (Leave Blank)	2. REPORT DATE April 1994	3. REPORT TYPE AND DATES COVERED Final Mar 92 – Jun 93

4. TITLE AND SUBTITLE	5. FUNDING NUMBERS
HIGH-EFFICIENCY ELECTRO-OPTIC GRATING ON PLZT CERAMIC WAFER FOR OPTICAL SWITCHING	C - F30602-92-C-0036 PE - 62702F PR - 4600 TA - P3 WU - PE
6. AUTHOR(S) Q. Wang Song	

7. PERFORMING ORGANIZATION NAME(S) AND ADDRESS(ES)	8. PERFORMING ORGANIZATION REPORT NUMBER
Syracuse University Office of Sponsored Programs 113 Bowne Hall Syracuse NY 13244-1200	A2-1852

9. SPONSORING/MONITORING AGENCY NAME(S) AND ADDRESS(ES)	10. SPONSORING/MONITORING AGENCY REPORT NUMBER
Rome Laboratory (OCPB) 25 Electronic Pky Griffiss AFB NY 13441-4515	RL-TR-94-68

11. SUPPLEMENTARY NOTES

Rome Laboratory Project Engineer: Joanne H. Maurice/OCPB/(315) 330-7670

12a. DISTRIBUTION/AVAILABILITY STATEMENT	12b. DISTRIBUTION CODE
Approved for public release; distribution unlimited.	

13. ABSTRACT (Maximum 200 words)

A high diffraction efficiency electro-optic phase grating is fabricated by depositing transparent interdigital electrodes on a PLZT ceramic wafer. The underlying principle is the electrical field induced periodic change in refractive index of the wafer. The diffraction efficiency is controlled by an applied DC voltage. The zero-order light is completely shut off when the first-order diffraction reaches its maximum, with a voltage of 140V. The preliminary analysis and experimental results are provided. This device can be used as a voltage-controlled switch in optical interconnects.

14. SUBJECT TERMS		15. NUMBER OF PAGES 32
Electro-Optic Diffraction Grating, Electro-Optic Phase Grating, PLZT Electro-Optic Grating		16. PRICE CODE

17. SECURITY CLASSIFICATION OF REPORT UNCLASSIFIED	18. SECURITY CLASSIFICATION OF THIS PAGE UNCLASSIFIED	19. SECURITY CLASSIFICATION OF ABSTRACT UNCLASSIFIED	20. LIMITATION OF ABSTRACT UL

TABLE OF CONTENTS

i

LIST OF FIGURES

1. Introduction

High diffraction efficiency phase-only gratings are a very useful optical element widely used in many areas including spectroscopy, optical information processing[1], and optical interconnections[2,3]. In general, most of the gratings are fixed, meaning their diffraction efficiencies are not changeable. In the areas such as optical switching and adaptive processing, it is often desirable to have control over the diffraction efficiency. Electro-optical (E-O) diffraction gratings[4-6] offer a means to control the diffraction efficiency. However, most of the designs and demonstrations to date use either opaque piezoelectrical materials in a reflection scheme, or metallic electrodes on E-O materials. Their overall diffraction efficiency, and thus the controllability, cannot be high. An E-O phase grating on $LiNbO_3$ was recently demonstrated[3]. The voltage to make the zero order disappear is about 525 V. The lanthanum-modified lead zirconate titanate (PLZT) E-O ceramic is an attractive E-O material. The fabrication of variable focal length lens and dual focal point lens with transparent electrodes on PLZT have been reported[7,8]. In this research, we demonstrate a high diffraction efficiency E-O phase grating fabricated on a PLZT ceramic wafer. The even orders of diffraction can be turned on or off. The zero order transmitted light can be almost completely shut off, which means that the device can be used as an optical switch with a high on-off ratio. The required DC voltage to do so is 140 V.

The research results are better than what we anticipated in the original proposal. We proposed to used the electrical field induced index change to achieve optical switching by means

1

of total internal reflection. But along the research, we found that the switching on-off ratio based on total internal reflection cannot be high with all the existing electro-optical material. In addition, the exit angle of all the existing electro optical switch is close to 90 degrees which makes the application of the switching impractical. Our newly designed electro optical diffraction grating has a near 100 percent diffraction efficiency. It can be used as a coupling switch in guided-wave optical interconnection.

The organization of the report is as follows. Section 2 gives the background of the electro optical material we used, including its properties and advantages as compared with other existing electro optical materials. Section 3 details the operation principle of electro optical grating we fabricated and tested. Section 4 presents the simulation results based on the theories developed in the previous section. An experimental set up and measurement results supporting our theory are also provided in this section. The summary section recaps the major contribution of this effort. Some suggestions for future research to advance this topic are given. This is followed by the references used in the project.

2. PLZT Electro Optic Ceramic Wafer

The lanthanum-modified lead zirconate titanate (PLZT) ceramic wafer is a relatively new type of electro-optic material. Different from the electro-optic single crystals, the PLZT does not have a very regularly periodic lattice structure. However, when an external electrical field is applied, the electrons in the material redistribute, and the material exhibits an induced structural regularity and hence birefringence. There exists numerous E-O materials. We chose PLZT ceramic wafer as the E-O substrate because it has some unique advantages making it preferable

2

to other E-O materials. PLZT belongs to ferroelectric materials that possess a spontaneous dipole which is reversible by an applied electrical field[9]. Its attractive features include high quadratic E-O coefficients, good optical transparency, high electrical resistivity, and moisture insensitivity. PLZT has a number of properties that can complement the ferroelectric liquid crystal and single crystal in engineering applications. For instance, PLZT has better mechanical and temperature stabilities than ferroelectric liquid crystals. When compared with E-O single crystals, PLZT is much more affordable and realistic when large-sized wafers with uniform optical and E-O properties are required. The key features to our interests are listed as the following:

1 - Ceramics can be hot pressed into any size or shape, whereas single crystals must be grown in some fixed crystallographic orientation which restricts their size and shape.

2 In general, ceramics are much less expensive than the single crystals.

3 - The optical axis and birefringence of E-O ceramics are controlled by the direction and the strength of the applied strength of the applied electrical field, whereas the single crystals have fixed optical axis, which limits the flexibility.

4 - E-O properties of ceramics may be tailored according to the application whereas it is difficult to do this in single crystals.

Because of these advantages, the PLZT has drawn attention in the optical community.

3

Some of its applications, such as pilot eye goggle and high-speed optical shutter, are already used in the military.

3. Principle of Operation

The structure of the PLZT ceramic wafer based E-O phase grating is shown in Fig. 1. The transparent indium tin oxide (ITO) interdigital electrodes are on one side of the wafer. The grating is made by first coating a thin film of ITO onto the wafer using sputtering deposition, and then using the standard photo lithographic procedure with dry ion etching to generate the designed grating. The fabricated grating has a spatial period of 200 microns with half of it occupied by the electrode, which has a thickness of about 1000 Angstroms. Since the index of refraction for the ITO film is around 1.8, the electrodes produce an intrinsic grating with a phase modulation of about one third of a wavelength for He-Ne laser.

The underlying principle of the E-O phase grating is that the applied E-field induces a periodic distribution of the index of refraction through quadratic E-O effect. The principle of operation can be understood by using linear approximation of the E-field inside the PLZT wafer. The side view structure of the E-O grating is shown by Fig. 2(a). There exists an intrinsic grating structure due to the finite thickness of the ITO electrodes. Upon the application of voltage between the adjacent electrodes, the E-field inside the PLZT wafer can be approximated as depicted by the E-field lines in Fig. 2(a). PLZT is a negative birefringent material. Since the transverse E-field is mainly between the electrodes, the index of refraction of PLZT in the central regions between the electrodes is modulated to a smaller value, while that in the regions right behind the electrodes is roughly unchanged. This periodic modulation of refractive index gives

4

rise to an induced phase grating. The total effective grating is the combination of the intrinsic grating and the E-field induced grating.

The voltage-induced phase profile can be obtained by calculating the electrical field inside the wafer and then using the method of index ellipsoid. The voltage distribution in the wafer can be expressed by

$$V(x,y) = \sum_{m=1}^{\infty} B_m \sin\left(\frac{m\pi x}{b}\right)e^{-m\pi y/b} \tag{1}$$

The potential is assumed to satisfy an ideal periodic linear boundary condition, namely,

$$V_0(x,0)= \begin{cases} -\dfrac{vx/2}{b/4} & 0\leq x\ \mathrm{mod}(2b)<b/4 \\[2mm] -\dfrac{v}{2} & b/4\leq x\ \mathrm{mod}(2b)<3b/4 \\[2mm] -\dfrac{v}{2}+\left(\dfrac{v/2}{b/4}\right)(x-\dfrac{3b}{4}) & 3b/4\leq x\ \mathrm{mod}(2b)<5b/4 \\[2mm] \dfrac{v}{2} & 5b/4\leq x\ \mathrm{mod}(2b)<7b/4 \\[2mm] \dfrac{v}{2}-\left(\dfrac{v/2}{b/4}\right)(x-\dfrac{7b}{4}) & 7b/4\leq x\ \mathrm{mod}(2b)<2b \end{cases} \tag{2}$$

The coefficients of the periodic sum are computed by sine transforms

$$B_m=\frac{1}{b}\int_0^{2b} V_0(x,0)\sin\left(\frac{m\pi x}{b}\right)dx. \tag{3}$$

The electric field is obtained as the negative gradient of the electric potential, with the x and y components given by

$$E_x(x,y) = -\sum_{m=1}^{\infty} B_m(\frac{m\pi}{b})\cos(\frac{m\pi x}{b})e^{-m\pi y/b} \qquad (4)$$

$$E_y(x,y) = \sum_{m=1}^{\infty} B_m(\frac{m\pi}{b})\sin(\frac{m\pi x}{b})e^{-m\pi y/b} \qquad (5)$$

The magnitude of the E-field is

$$E(x,y) = \sqrt{E_x^2(x,y) + E_y^2(x,y)} \qquad (6)$$

The PLZT wafer used in the experiment has a 65/35 ratio of $PbZrO_3$ to $PbTiO_3$ with a Lanthanum concentration of 9.5%. It is conventionally designated as PLZT (9.5/65/35). The wafer is isotropic when no external E-field is present. Under an applied electric field, the wafer exhibits a transition from an optically isotropic cubic phase to a rhombohedral or tetragonal ferroelectric phase with an quadratic optical anisotropy. The induced index ellipsoid is uniaxial with the optical axis oriented parallel to the applied electric field [9]. The ellipsoid is expressed by

$$(\frac{1}{n_1^2(x,y)})\ x^2 + (\frac{1}{n_2^2(x,y)})\ y^2 + (\frac{1}{n_3^2(x,y)})\ z^2$$
$$+ (\frac{1}{n_4^2(x,y)})\ yz + (\frac{1}{n_5^2(x,y)})\ zx + (\frac{1}{n_6^2(x,y)})\ xy = 1 \qquad (7)$$

When the applied E-field is zero, the above equation degenerates into a spherical surface with $n_1(x,y) = n_2(x,y) = n_3(x,y) = 2.5$, and $n_4(x,y) = n_5(x,y) = n_6(x,y) = 0$.

Thus the electro-optically induced perturbation in the index ellipsoid of PLZT (9.5/65/35) can be derived by the following isotropic quadratic electro-optic tensor equation.

$$
\begin{bmatrix}
\Delta(\dfrac{1}{n_1^2(x,y)}) \\[2ex]
\Delta(\dfrac{1}{n_2^2(x,y)}) \\[2ex]
\Delta(\dfrac{1}{n_3^2(x,y)}) \\[2ex]
\Delta(\dfrac{1}{n_4^2(x,y)}) \\[2ex]
\Delta(\dfrac{1}{n_5^2(x,y)}) \\[2ex]
\Delta(\dfrac{1}{n_6^2(x,y)})
\end{bmatrix}
=
\begin{bmatrix}
R_{11} & R_{12} & R_{12} & 0 & 0 & 0 \\
R_{12} & R_{11} & R_{12} & 0 & 0 & 0 \\
R_{12} & R_{12} & R_{11} & 0 & 0 & 0 \\
0 & 0 & 0 & R_{44} & 0 & 0 \\
0 & 0 & 0 & 0 & R_{44} & 0 \\
0 & 0 & 0 & 0 & 0 & R_{44}
\end{bmatrix}
\begin{bmatrix}
E_x^2(x,y) \\
E_y^2(x,y) \\
E_z^2(x,y) \\
E_y(x,y)E_z(x,y) \\
E_z(x,y)E_x(x,y) \\
E_x(x,y)E_y(x,y)
\end{bmatrix}
\qquad (8)
$$

After some mathematical manipulations, the new principle axes at an arbitrary location inside the wafer are expressed as

$$
n_{x'}(x,y) = n_0 - \frac{1}{2}n_0^3 R_{11} E^2(x,y) \qquad (9)
$$

$$
n_{y'}(x,y) = n_0 - \frac{1}{2}n_0^3 R_{12} E^2(x,y) \qquad (10)
$$

$$
n_{z'}(x,y) = n_0 - \frac{1}{2}n_0^3 R_{12} E^2(x,y) \qquad (11)
$$

where x', y', and z' denote the new principal coordinates as illustrated in Fig. 2(b). Notice $n_{x'}(x,y)$ is the extraordinary refractive index, and $n_{y'}(x,y)$ and $n_{z'}(x,y)$ are the ordinary ones. Therefore, the refractive index for ordinary light, whose polarization is parallel to the electrodes, is $n_{z'}(x,y)$. The refractive index for light polarized perpendicularly to the electrodes is $n_e(\theta(x,y))$. It is calculated by

7

$$\frac{1}{n_e^2(\theta(x,y))} = \frac{\cos^2(\theta(x,y))}{n_{z'}^2(x,y)} + \frac{\sin^2(\theta(x,y))}{n_{x'}^2(x,y)} \qquad (12)$$

where $\theta(x,y)$ is the angle between x and x' axes as shown in Fig. 2(b).

With the induced refractive indices available, the effective light path modulations of the light transmitted through the wafer for the two eigen polarizations can be obtained through

$$\Delta\phi_\parallel(x) = \int_0^d n_{z'}(x,y)dy \qquad (13)$$

$$\Delta\phi_\perp(x) = \int_0^d n_e(\theta(x,y))dy \qquad (14)$$

where the parallel and perpendicular subscripts denote the polarizations parallel and perpendicular to the orientation of the ITO electrodes, respectively, and d is the thickness of the PLZT wafer. This transmitted light also experiences the light path modulation by the ITO electrodes due to their finite thickness. This intrinsic modulation can be calculated by

$$\Delta\phi_{ITO}(x) = \begin{cases} d_{ITO} & 0 \le x \bmod (b) < b/4 \\ n_{ITO}d_{ITO} & b/4 \le x \bmod (b) < 3b/4 \\ d_{ITO} & 3b/4 \le x \bmod (b) < b \end{cases} \qquad (15)$$

where d_{ITO} is the thickness and n_{ITO} is the refractive index of the ITO electrodes. The total effective grating is the combined phase delays of the intrinsic grating and the induced one.

Based on the above analysis, the transmitted optical waves for the two eigen polarizations emerging from the electro-optic PLZT/ITO phase grating are expressed in terms of the effective

8

phase delays

$$E_{\parallel}(x) = \exp\left\{-j\frac{2\pi}{\lambda}[\Delta\phi_{\parallel}(x) + \Delta\phi_{ITO}(x)]\right\}$$ (16)

$$E_{\perp}(x) = \exp\left\{-j\frac{2\pi}{\lambda}[\Delta\phi_{\perp}(x) + \Delta\phi_{ITO}(x)]\right\}$$ (17)

Finally, the far-field diffraction for the two eigen polarizations are calculated by Fourier transforming the above two equations. Note that when the applied voltage changes, the effective phase modulations of the grating, and thus the far field diffraction, will be changed.

4. Computer Simulation and Experimental Results

We simulated the far-field diffraction of the PLZT grating under some specific voltages used in the experiment. The polarization perpendicular to the electrodes experiences larger modulation since it makes use of the larger diagonal Kerr coefficient. Therefore, we just present the results for light polarized perpendicularly to the electrodes. The refractive index of ITO is taken to be 1.775. The numerical values of the Kerr coefficients in the literature are $R_{ii}=4.00\times10^{-16}m^2/V^2$ [10], $R_{ij}=2.42 \times 10^{-16}$ m^2/V^2 [8]. We found that when using $R_{ii}=3.00\times10^{-16}m^2/V^2$ and $R_{ij}=2.42 \times 10^{-16}$ m^2/V^2, the computer simulation produced results that have very good match with the experimental results.

Fig. 3 shows the simulation results of normalized far field diffraction under different applied voltages. Note that the horizontal axis is of arbitrary unit. Therefore, only the relative spacings among the diffraction orders are meaningful. Fig. 3(a) is the diffraction without applied voltage. The even orders are not present because the width of the electrodes is half of the grating

period. When the applied voltage is 75 V, the zero order is decreased and first orders are increased to an equal value, as shown in Fig. 3(b). Fig. 3(c) is the diffraction pattern for voltage of 140 V. Note that now the zero order is completely shut out and the even orders appear. This means that the induced grating has the same period of the intrinsic grating but the modulation depth and width are varied. Further increasing the voltage to 175 V will bring back the zero order while further increasing the value of all higher odd and even diffracted orders.

The experimental set up for measuring the diffraction of the E-O grating is depicted by Fig. 4. The grating is set on a rotatable stage. The flat side of the PLZT wafer (i.e., without ITO electrodes) faces the incident light. The polarization of the incident light is controlled by a polarizer/compensator combination. The transmitted and reflected diffraction patterns are scanned by a linearly moving slit, which is 100 μm wide with orientation perpendicular to the scanning direction. A photodetector is mounted on the back of the slit. The output from the photodetector is sent to a digital memory oscilloscope to show and plot the scanned results.

Figure 5 shows the measured change of transmitted diffraction with different applied voltages. Figure 5(a) is the diffracted pattern of the intrinsic grating due to the finite thickness of the ITO electrodes. No even orders are present because the width of the electrodes equals a half period. As the voltage increases, the induced grating increases the modulation of the total effective grating and thus more energy is diffracted. At 75 V, the zero order has decreased and first-orders have increased to an equal intensity as shown in Figure 5(b). At 140 V, most of the incident light is diffracted such that the zero order is almost zero and the first orders take their maximum as given in Figure 5(c). The ratio of this first-order peak intensity to the zero-order intensity without the applied voltage is about 5/8. This means that an extremely high diffraction

efficiency can be achieved by this grating. Further increase of the voltage will bring the zero order back as shown by Figure 5(d). The experimental results of the diffraction have the exact behavior as predicted by the simulation given in Fig. 3.

This grating produces about sixty diffracted high orders. They are much weaker than the first order. The changes of diffraction of the higher orders are shown in Fig. 6. Figure 6(a) is the diffraction pattern with no applied voltage. The even orders start to appear when the voltage is 75 V as shown in Figure 6(b). This behavior clearly indicates that the spacing ratio of the induced grating is not the same as that of the intrinsic ITO grating which has a spacing ratio of one. The intensities of all high orders (except the third one) are dramatically increased when higher voltages are applied, as shown in Figure 6(c) and Figure 6(d). It is interesting to point out that the gains of diffraction efficiencies for different orders are not uniform as the voltage increases. The summed power of all the transmitted orders is about 65% of the incident power. This is because the PLZT has a high refractive index of 2.5. The front surface reflection accounts for about 20% of the energy loss. The reflection and reflected diffraction on the back surface further take away the incident energy. We believe an anti-reflection coating will be able to largely reduce the reflection loss. The relationship of relative gains of different orders are under study.

Figure 7 shows the influence of the voltage to the reflected diffraction. The diffraction of the intrinsic grating is very weak. This is because the reflection coefficients of both front and back surfaces are about 0.4 due to the large index of refraction of PLZT and the reflected diffraction of the intrinsic grating which is low due to its low modulation has to suffer the loss three times (twice at the back and once at the front surfaces). At 140 V, a clear diffraction

11

pattern is generated, as shown by Figure 7(a). Just like the transmitted light, the higher orders are much weaker than the first order. The detail of these orders are given in Fig. 7(b). Except for the second order, the higher even orders are a bit stronger than the odd orders. This is in contrast with that of the transmitted light as given in Fig. 7(c). More interestingly, the first three odd orders are dramatically suppressed with a high voltage as shown in Fig. 7(c) and Fig. 7(d), respectively. Note that the first order is completely shut off. This may be useful in certain switching applications. We think the reflected diffraction arises from the double pass through the wafer with the reflection from the back surface.

All above results are for light polarized perpendicularly to the electrodes. For light polarized parallel to the electrodes, similar results are obtained but with lower efficiencies. This phenomenom is due to the fact that the diagonal tensor element of PLZT is smaller than the off diagonal ones. Therefore, the phase modulation for the X polarization is weaker than that for the Z polarization as depicted by Eqs. 9 and 11, respectively. The diffraction is not sensitive to the incident angle, indicating that the grating is still a thin one. This means that the E-field penetration into the wafer is shallow.

5. Summary

In conclusion, we have fabricated a high efficiency E-O grating on a PLZT wafer. The applied voltage controls the gains of diffracted orders nonuniformly. The operation can be explained by the E-field induced grating in the negative birefringent material. This grating can be used as the coupling switch for guided-wave reconfigurable interconnection, controllable free-space optical fan-in fan-out devices, or an adaptive device in multichannel optical processing.

The intrinsic gr   due to the finite thickness of the ITO electrodes may or may not cause problems depending on the applications. It can be removed by merging the electrodes in an index-matching liquid. The time response (RC constant) of the grating depends on its size. Our calculation shows it is on the order of a microsecond for a 1 cm^2 grating. This estimation is not experimentally verified due to the lack of an adequate voltage supply in the laboratory. Detailed analysis of the E-field induced diffraction is under way.

References

1. Francis T. S. Yu, *Optical Information Processing*, Wiley Inc., New York, 1983.

2. Q. Wang Song, Francis T. S. Yu, Appl. Opt., Vol. 27, PP.1222-1223 (1988).

3. R. T. Chen, D. Robinson, H. Lu, M.R. Wang, T. Jannson, R. Baumbick, Opt. Eng., Vol. 31, PP.1098-1105 (1992).

4 J. M. Hammer, Appl. Phys. Lett., Vol. 18, PP.147-149 (1971).

5. H. Sato, K. Toda, J. Appl. Phys., Vol. 47, PP.4031-4032 (1976).

6. T. Utsunomiya, H.Sato, Ferroelectrics, Vol. 27, PP.27-30 (1980).

7. T. Tatebayashi, T. Yamamoto, and H. Sato, Appl. Opt., Vol.30, PP.5049-5055 (1991).

8. T. Tatebayashi, T. Yamamoto, and H. Sato, Appl. Opt., Vol.31, PP.2770-2775 (1992).

9. G. Haertling, in *Electronic Ceramics*, L. Levinson, ed., PP.371-492, Marcel Dekker Inc., New York, 1988.

10. G. Heartling, in chapter 8 of *Ceramic Materials for Electronics*, B. C. Buchanan ED., Marcel Dekker Inc., New York, 1986.
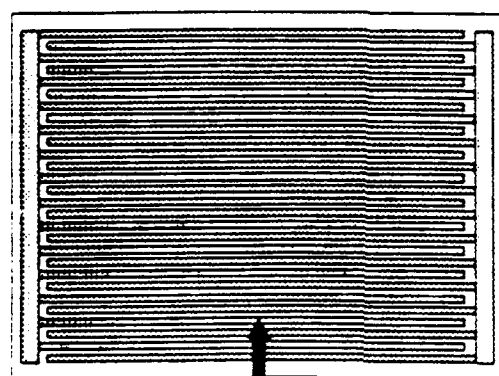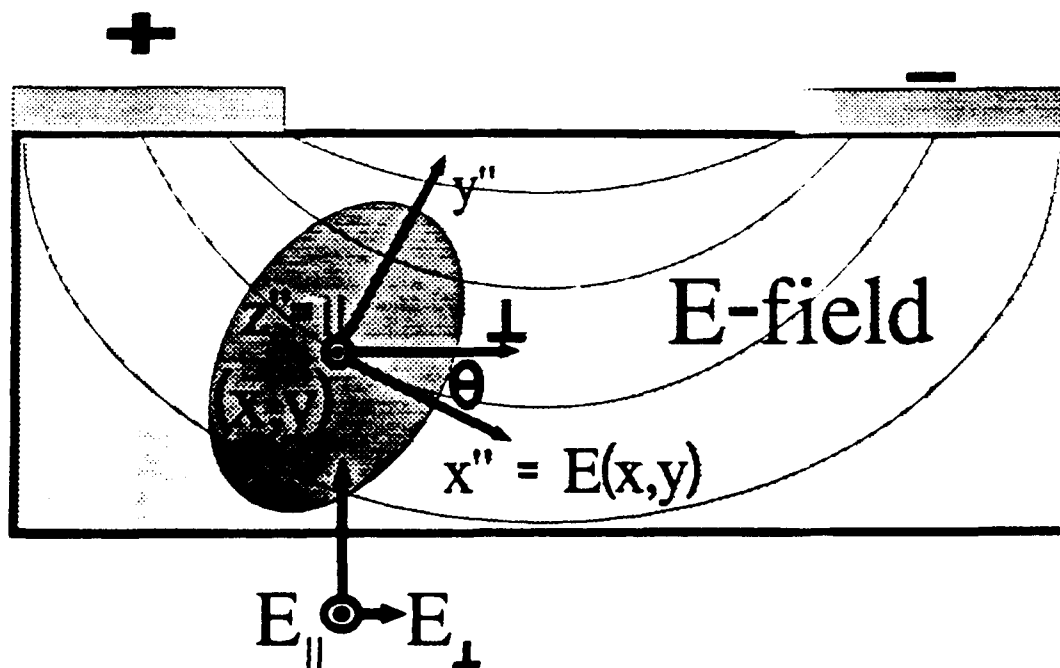
Fig. 1. PLZT wafer based E-O phase grating.
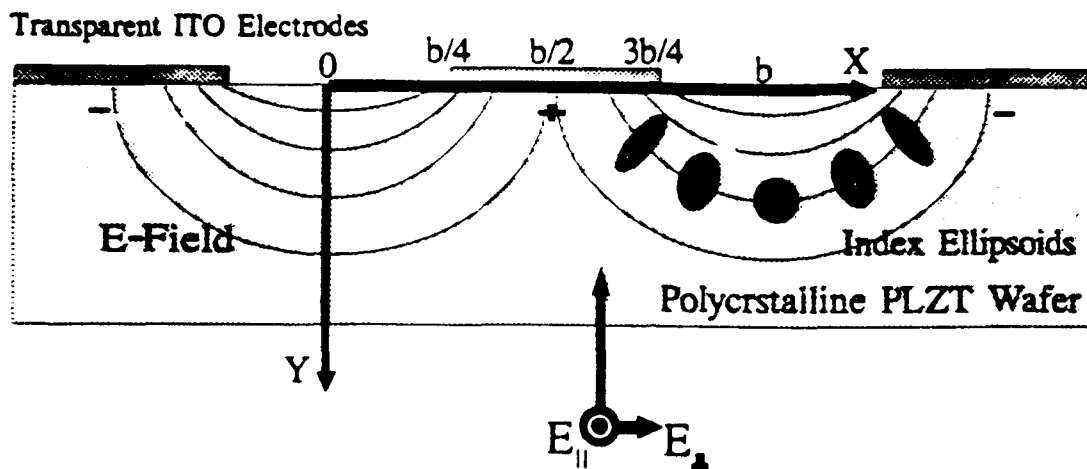
Fig. 2. Structure and the principle of the E-O grating: (a) side view structure; (b) portion of (a) with induced index ellipsoid and its new principal axes.
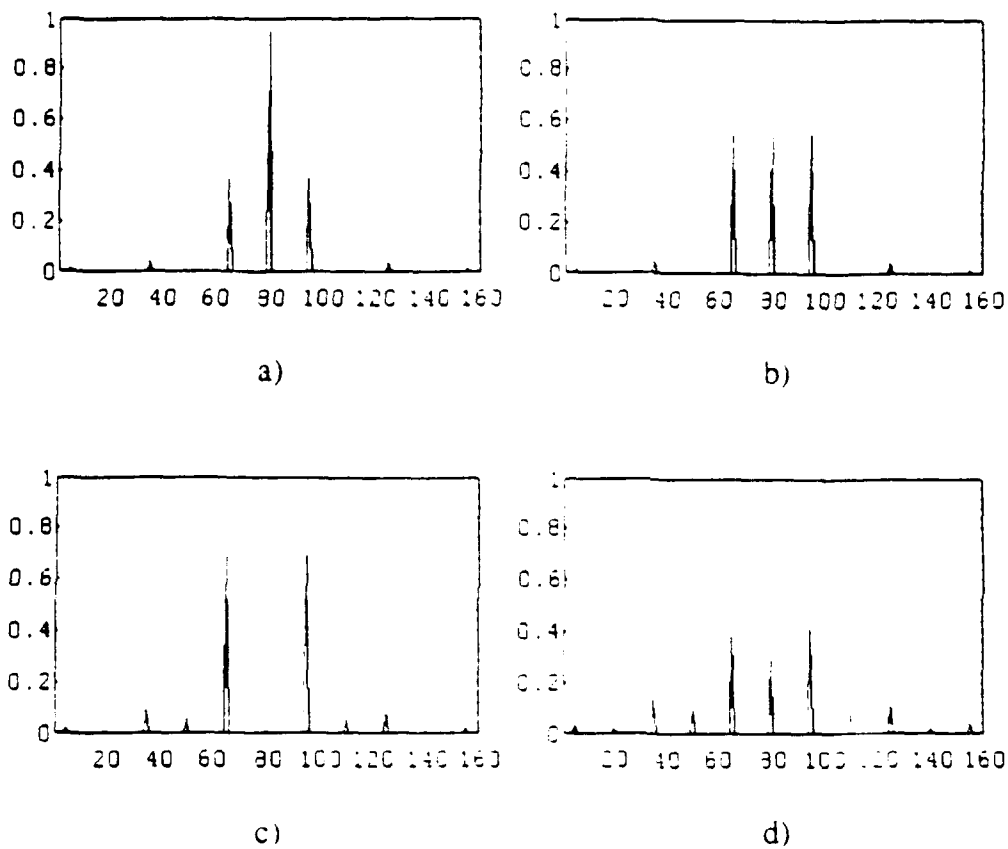
Fig. 3. Simulation of normalized far field diffraction with horizontal axis being of arbitrary spatial frequency unit; (a) the diffraction due to intrinsic grating of ITO electrodes; (b) diffraction when the applied voltage is 75 V; (c) diffraction when the applied voltage is 140 V; (d) diffraction when the applied voltage is 175 V.
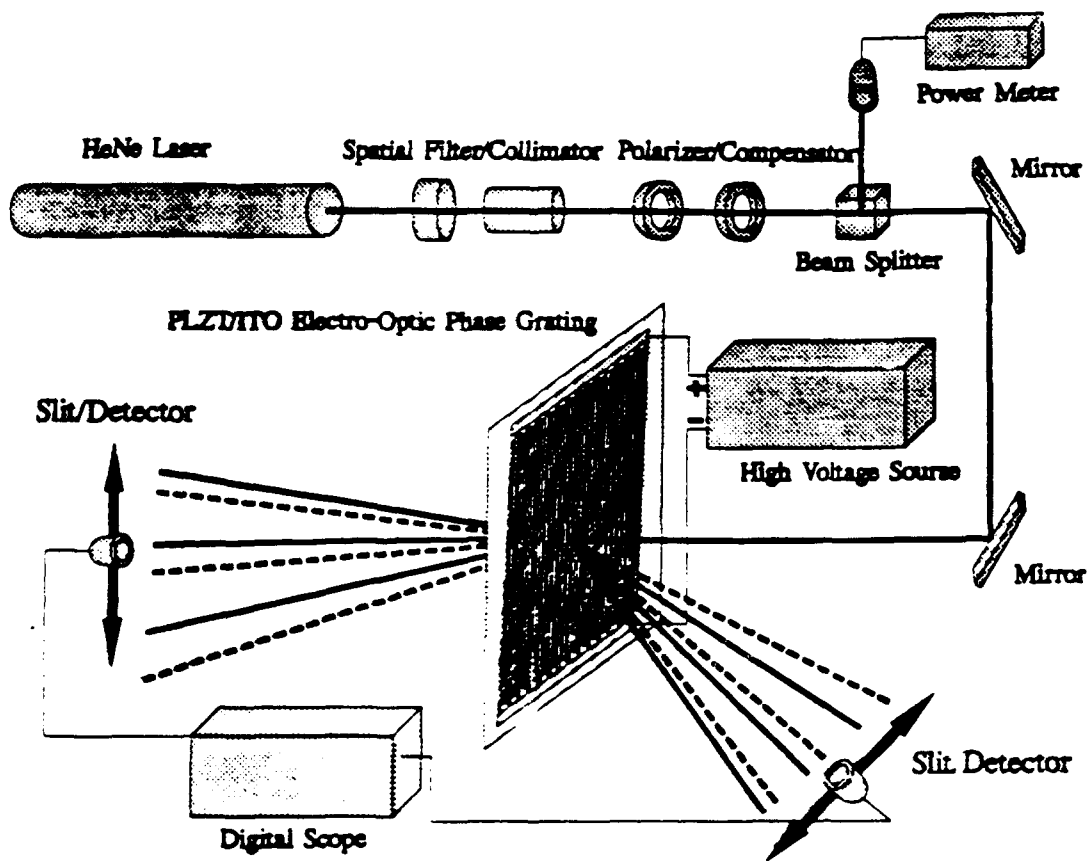
17

Fig. 4. Experimental set up to measure the diffraction of the E-O grating. The Polarizer/Compensator controls the polarization of the incident light. Both of the Slit/Detectors are mounted on one-dimensional linearly moving stages.
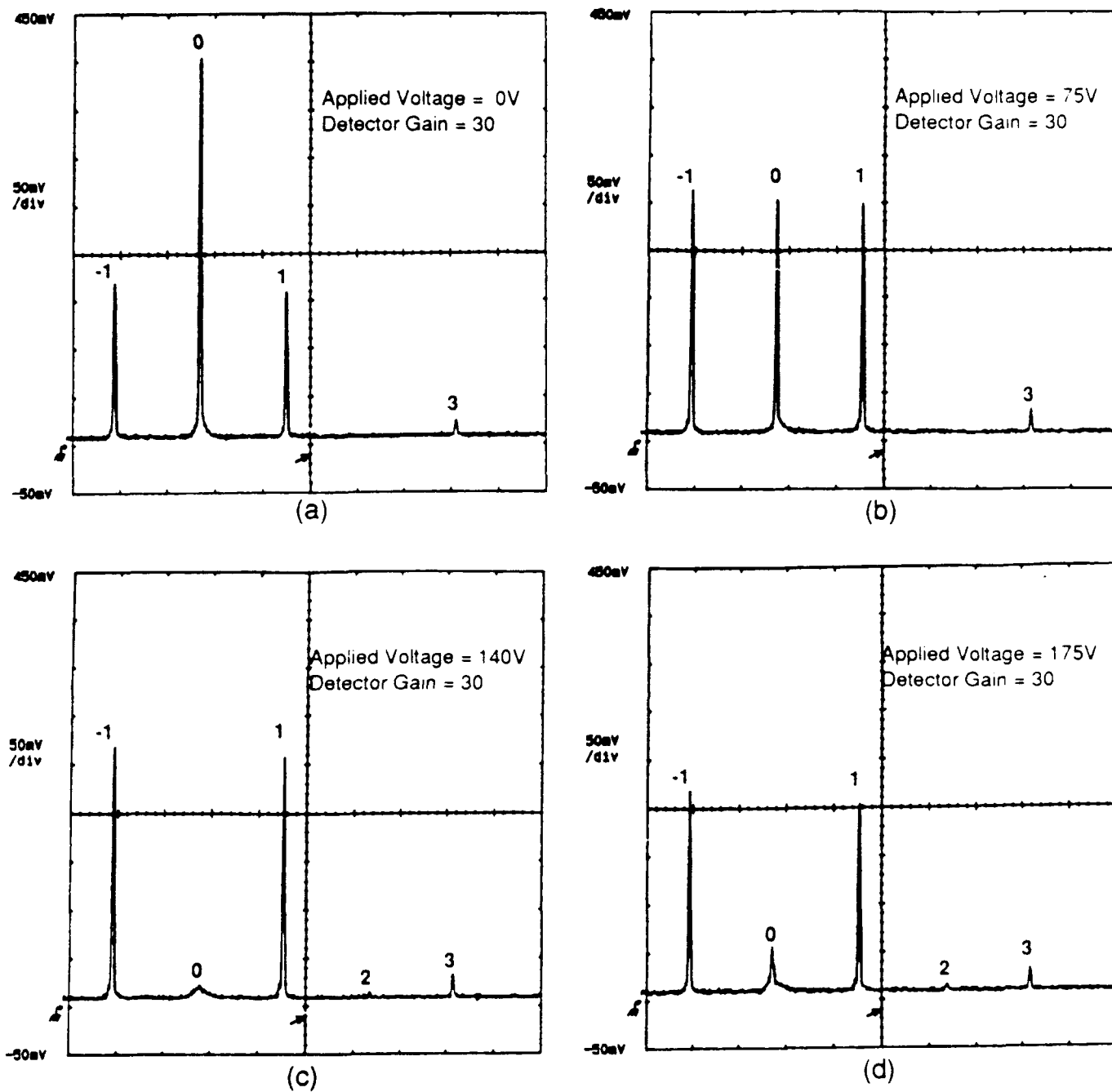
Fig. 5. Measured diffraction patterns of the transmitted light under different applied voltages with the gain of the detector shown in each measurement plot.
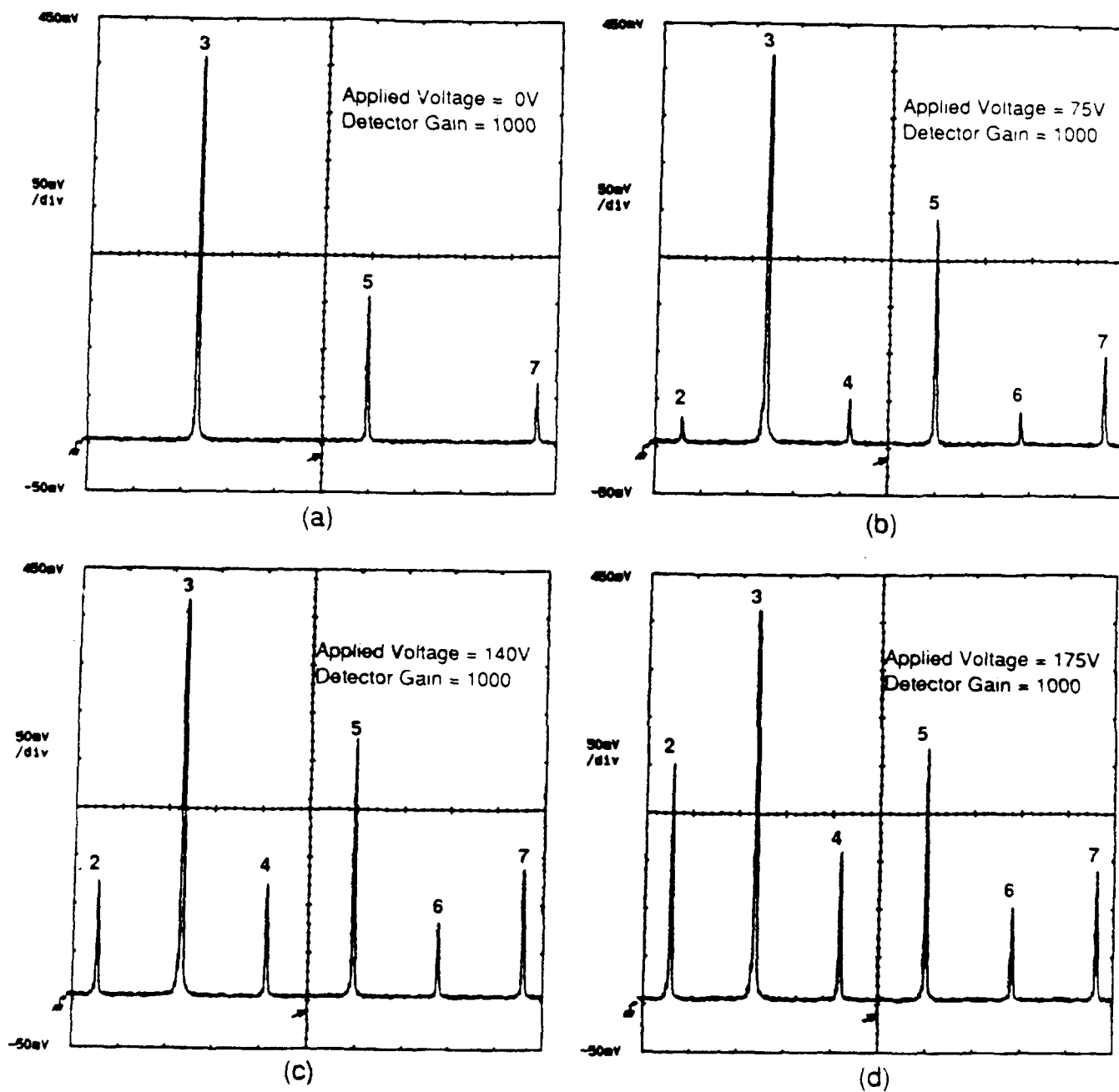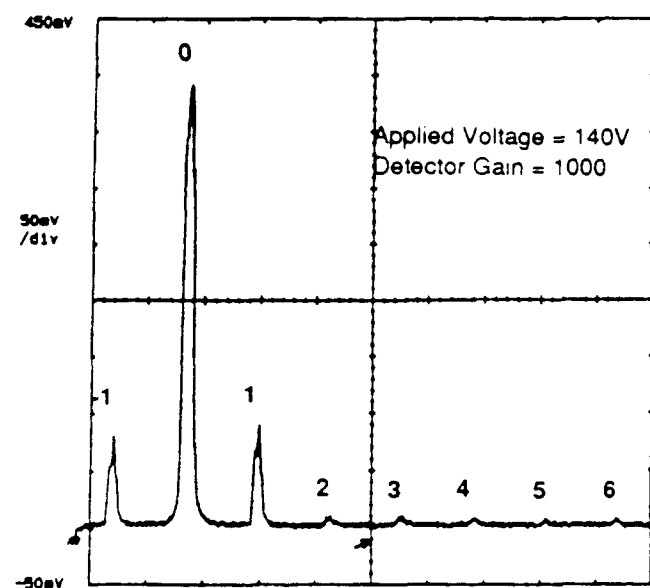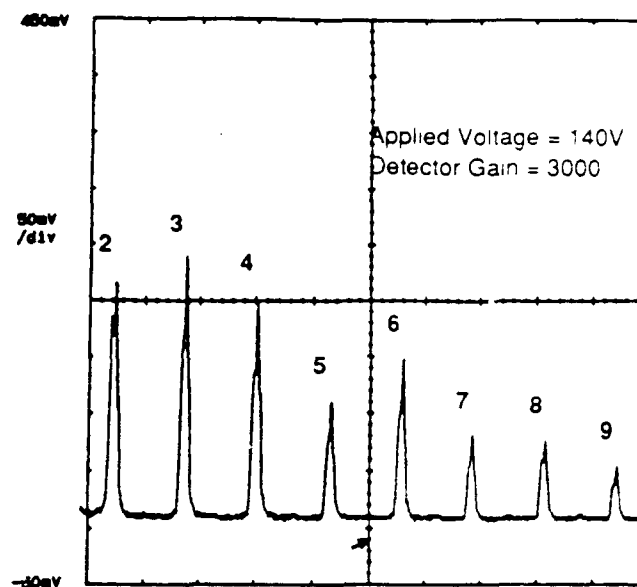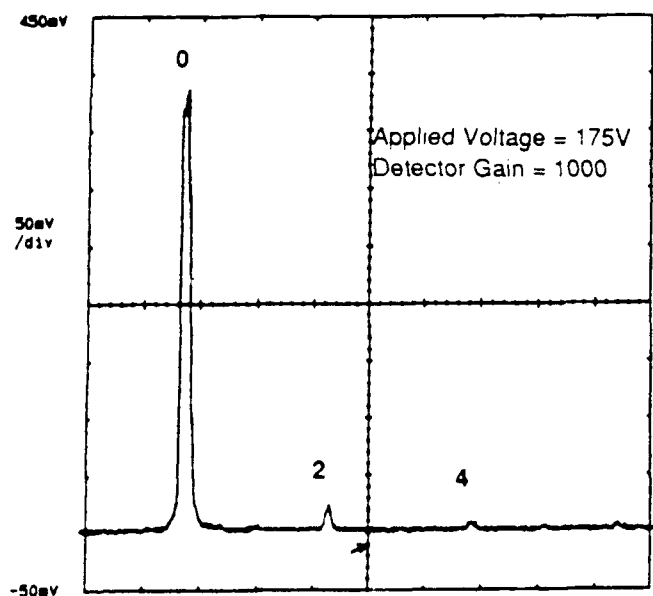
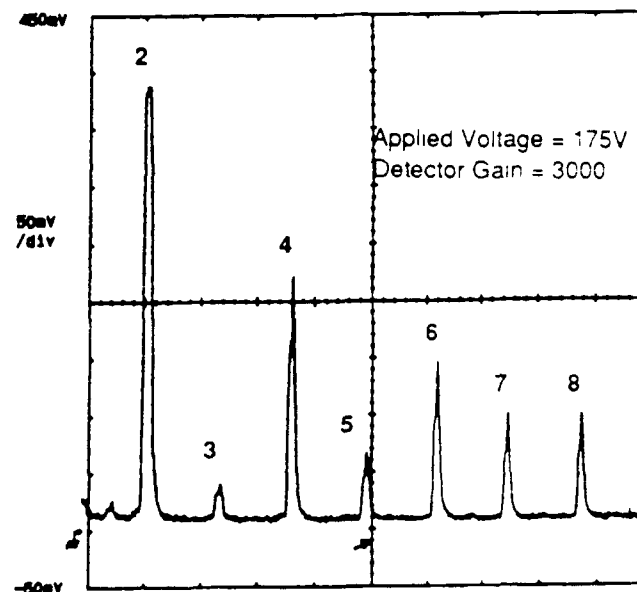Fig. 6. Diffracted high orders of transmitted light under different applied voltages.

(a)

450mV

0

Applied Voltage = 140V
Detector Gain = 1000

50mV
/div

-1   1

2   3   4   5   6

-50mV

(b)

450mV

Applied Voltage = 140V
Detector Gain = 3000

50mV
/div

2   3
         4
                    6
              5   7   8
                                      9

-50mV

(c)

450mV

0

Applied Voltage = 175V
Detector Gain = 1000

50mV
/div

2   4

-50mV

(d)

450mV

2

Applied Voltage = 175V
Detector Gain = 3000

50mV
/div

              4
                          6
                                7   8
       3   5

-50mV

Fig. 7. The influence of applied voltage to the reflected diffraction.

21

MISSION

OF

ROME LABORATORY

Mission. The mission of Rome Laboratory is to advance the science and technologies of command, control, communications and intelligence and to transition them into systems to meet customer needs. To achieve this, Rome Lab:

    a. Conducts vigorous research, development and test programs in all applicable technologies;

    b. Transitions technology to current and future systems to improve operational capability, readiness, and supportability;

    c. Provides a full range of technical support to Air Force Materiel Command product centers and other Air Force organizations;

    d. Promotes transfer of technology to the private sector;

    e. Maintains leading edge technological expertise in the areas of surveillance, communications, command and control, intelligence, reliability science, electro-magnetic technology, photonics, signal processing, and computational science.

The thrust areas of technical competence include: Surveillance, Communications, Command and Control, Intelligence, Signal Processing, Computer Science and Technology, Electromagnetic Technology, Photonics and Reliability Sciences.